Wireless biosensors for POC medical applications

7

M.S. Arefin, J.-M. Redouté, M.R. Yuce
Monash University, Melbourne, VIC, Australia

7.1 Introduction

Point of care (POC) biosensor systems which do not rely on the use of laboratory staff or facilities have the potential to improve patient health care [1]. POC system contains different types of wearable or implantable biosensors, readout or interface circuits, power management circuits, and wireless telemetry blocks. A typical POC system is depicted in Fig. 7.1. The system contains several biosensors with analog readout circuits, a digital microcontroller, a radio transmitter, and a battery. The sensors convert the physiological parameters to electrical quantities with readout circuits. The digital microcontroller circuit manages and processes all the sensor data. The data are then transmitted using a wireless transmitter to an external device for remote monitoring and recording.

Wireless POC systems provide the means to continuously measure and monitor biological parameters related to diseases, biomolecules, and pathogenic bacteria and viruses. Diseases like diabetes, ischemia, Alzheimer's, and epilepsy require continuous monitoring and real-time drug delivery system or stimulation. There are many biosensors reported for measuring and detecting biological parameters. These biosensors can be grouped into two categories of POC biosensors, namely, implantable biosensors and wearable biosensors.

Implantable biosensors are continuously becoming more popular and economically viable. In the past, the main contribution in this field was to restore malfunctioning or missing biological structures by artificial prosthetic devices such as an artificial heart and pacemaker for cardiac patients, a neurostimulator for patients with epilepsy and Alzheimer's, stents for damaged arteries, and knee implants for rheumatoid arthritis, osteoarthritis, or traumatic injuries. These biosensors offer improved quality of life

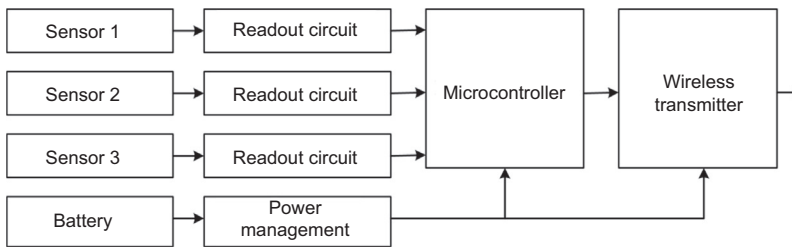

Figure 7.1 A wireless point of care system with integrated biosensors and readout circuits.

Medical Biosensors for Point of Care (POC) Applications. http://dx.doi.org/10.1016/B978-0-08-100072-4.00007-1

for patients. As an extension to this field, miniaturized implantable biosensors are also directed toward the diagnosis of diseases with higher measurement sensitivity and selectivity of physiological parameters [2]. These biosensors provide continuous diagnostics for patients with chronic diseases. The integration of wireless capability with these sensors enables health condition monitoring in real-time as well as real-time drug delivery systems. The continuous glucose-monitoring system, developed by Medtronic, can measure glucose level more than 200 times a day, and the insulin delivery system provides an alternative to multiple daily injections [3,4]. The bladder pill is developed to monitor and log the internal bladder pressure: it is inserted into the bladder cavity through a minimally invasive procedure [5]. The pressure sensor and readout circuit are packaged in a flexible pill-shaped form, having a length of 40 mm and diameter of 5 mm. The continuous measurement of the physiological parameters in the gastrointestinal (GI) tract is often necessary for detecting and monitoring abnormalities [6]. Traditionally, the diagnosis of the GI abnormalities is performed by inserting a tube containing sensors through the mouth [6]. This time-consuming and uncomfortable method for patients has motivated researchers to develop wireless capsules by integrating miniature sensors including pH, pressure, and temperature onto a single platform. The integration of biosensors and integrated circuit (IC) technology with a wireless link forms the basis for future multisensor microsystems and leads to real-time and continuous monitoring of the GI tract.

Extensive research has been performed in the field of wearable biosensors for continuously monitoring health, activity, mobility, and biopotentials. The major monitoring of vital signs are the electrocardiogram (ECG) for measuring cardiac electrical activity and heart sounds, the electromyogram (EMG) for measuring muscular electrical activity, the electroencephalogram (EEG) for measuring the electrical activity of the brain, respiration rate, mobility for limb movement, skin temperature, electrical conductivity of skin, and blood glucose [7]. The biosensors for monitoring these vital signs are embedded in the user's outfit. For example, a wrist-worn device has been developed to monitor ECG, blood pressure, blood oxygen saturation, acceleration, and temperature by combining all sensors, signal processing, and cellular communication [8]. The communication protocol has been designed to support cellular message service to transmit a small number of values, a virtual circuit switched communication channel for long ECG data, and an internet-based channel to reduce the number of direct lines needed at the telemedicine center. A portable physiological signal recorder is also designed and implemented to measure ECG, bioimpedance, and activity using Ag/AgCl gel-paste electrodes and three-axis acceleration sensors [7,9]. A textile-based wearable system has also been developed to monitor ECG, photoplethysmography (PPG), heart rate, blood pressure, body temperature, and skin conductance [10]. The data are sampled and digitized at 250 samples/s and transmitted wirelessly using 2.4 GHz industrial, scientific, and medical (ISM) band to a remote monitoring station [7,10].

Wireless biosensors for implantable or wearable sensors will be discussed in this chapter. The biosensors incorporating electrical measurements such as electrochemical transduction mechanism [potentiometric, amperometric, and field-effect transistor (FET)] and electrical transduction mechanism (resistance, capacitance, and inductance)

will be described in the second section. The interface circuit techniques to convert these electrical properties of the biosensor into voltage, frequency, or phase will also be reviewed briefly. A design example including a capacitive pH-sensor device that detects pH variations will be studied in this section. In the third section, wireless telemetry systems will be described. The applications of the wireless link for implantable or wearable sensors, such as implanted blood-glucose sensor, wireless capsule, and wireless wearable device will be explored in the fourth section. In the fifth section, we will conclude the chapter with some future trends involving biocompatible coatings, suitable packaging, and flexible IC.

7.2 Electrical measurements using biosensors

7.2.1 Biosensing techniques

Microelectromechanical systems (MEMS)-based biosensors are widely used in various biomedical and lab-on-a-chip (LOC) applications, such as chemical and biochemical sensing [11], protein and DNA biosensor array [12], drug screening [13], disease and pathogens diagnosis [13,14], and implantable devices [15,16]. The biosensors transform the changes in chemical and biological analytes including dissolved ions, pH, gases, body fluids, drugs, microbes, human cells, proteins, and nucleic acids into optical, electrochemical, or electrical equivalent of the changes using biologically sensitive elements. A biosensor system example is depicted in Fig. 7.2. The biosensors are usually composed of a biologically sensitive element or compound and a transducer. The biologically sensitive elements interact with the chemical and biological analytes, and the transducer transforms the interaction with the chemical and biological analytes into a measurable signal (optical, electrochemical, or electrical).

Biosensors are classified into two major categories: label-based and label-free sensing. Label-based sensing requires the labeling of target molecules with fluorescent dyes, chemiluminescence, or radioactive labeling using enzyme-linked immunoabsorbent assay [17–19]. These processes collect and attach the target molecules from heterogeneous samples, and hence the specificity of the biosensor is characterized by the

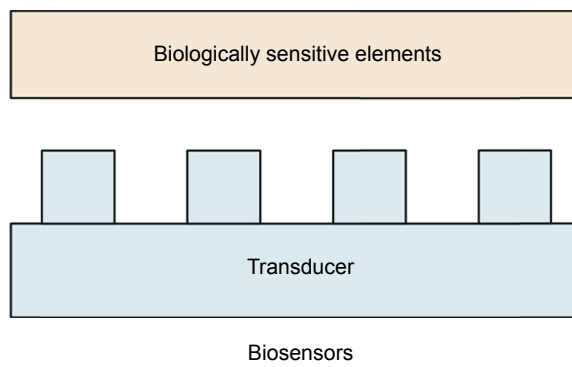

Figure 7.2 A biosensor system consisting of biologically sensitive elements and transducers.

sensing material. These labeling processes may interfere with the binding site, alter surface characteristics, and require a longer time [18]. These limitations may hinder the implementation of label-based sensing for POC applications. On the other hand, label-free sensing is based on the changes of inherent properties of test molecules [18,20]. In this method, the detection is typically performed on the chemical modification of the sensor's surface using the antibody, antigen, and μRNA [18,21,22]. Therefore, the selectivity and sensitivity are dependent on the quality of the surface-modification methods [21]. These methods aid in the development of biosensors for rapid detection with a higher sensitivity and selectivity. Hence, it is practical to implement the POC biosensors using label-free sensing mechanisms.

Apart from the classification based on sensing mechanisms, biosensors are classified into three categories considering the transduction mechanism used. They are optical, electrochemical, or electrical. The optical transduction mechanism includes fluorescence, chemiluminescence, interferometry, and surface plasmon resonance. These techniques involve either the production of light from chemical reactions or the change in refractive index at the interface of biosensing materials.

Electrochemical transduction mechanisms operate according to redox reactions involving the production of electrons or protons that can contribute to current or voltage. This method depends on the Nernstian response of redox reactions at solid–liquid interfaces and can achieve a maximum Nernstian sensitivity. This method is suitable when biochemical reactions between the biomolecules and biologically sensitive elements generate electrical charge. For example, glass electrode-based pH sensors detect pH levels in a sensing half-cell by measuring the voltage difference between the sensing electrode of the sensing half-cell and a reference electrode having a fixed concentration of HCl or a buffered chloride solution. The voltage difference is generated due to the exchange of sodium ions in the reference half-cell for H^+-ions in the sensing half-cell through a glass membrane [23]. There are different types of electrochemical biosensors: potentiometric, amperometric, and FETs. Potentiometric biosensors are based on the potential or voltage difference between the sensing and reference electrodes (Fig. 7.3(a)). This principle is widely used for pH-sensor and gas-sensor applications. Amperometric biosensors rely on the change in current between sensing and reference electrodes (Fig. 7.3(b)). For biosensors using FETs, the solutions are in contact with the gate of the transistor and the redox reaction produces the voltage at the gate that changes the current through the transistor (Fig. 7.3(c)). For the measurement of pH, ion-sensitive FETs (ISFETs) are widely used. An ISFET measures the current through a conduction channel between the source and the drain originating from pH-dependent threshold voltages due to sensing-gate liquid-surface potentials [24–27]. Different sensing materials at the sensing gate region, such as Si_3N_4, Al_2O_3, Pr_2O_3, InN, RuO_2, RuN, and Ta_2O_5 are used to achieve the theoretical upper limit of Nernstian sensitivity of 59.16 mV/pH [25–27]. The techniques utilizing electrochemical transduction are summarized with some design examples in Table 7.1.

The transducers producing electrical equivalents of the changes in passive components are suitable for miniaturized systems, which translate the changes in chemical and biological analytes into resistive, piezoelectric, capacitive, or inductive variations. Such methods are suitable for detecting biomolecules without biochemical reactions

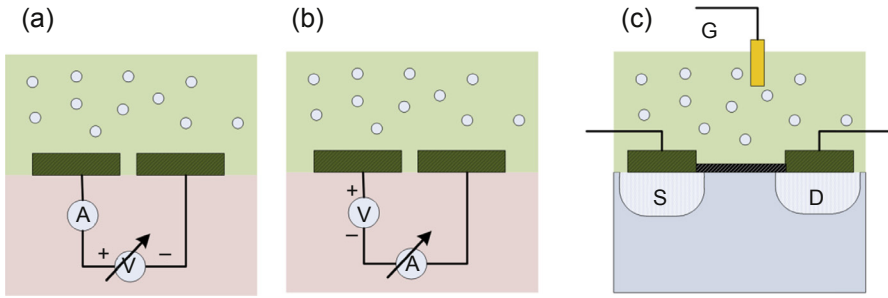

Figure 7.3 Electrochemical transduction techniques: (a) potentiometric technique, (b) amperometric technique, (c) field-effect transistor (FET) technique.

Table 7.1 Examples of electrochemical transduction techniques

Technique	Output	Membrane	Application	References
Potentiometric	Voltage	Alkaline phosphatase	DNA	[28]
	Frequency	N-(2-ferrocene-ethyl) maleimide	DNA	[29]
	Voltage	Si_3N_4 and parylene	Potassium ferricyanide	[30]
	Voltage	Iridium oxide	pH of urine	[31]
Amperometric	Frequency	Polyimide	Protein	[32]
	Current	SU-8	Protein	[12]
	Current	Platinum/nitrogen-doped graphene	Glucose	[33]
	Current	Glucose oxidase	Glucose	[34]
ISFET	Voltage	Indium nitride (InN)	pH	[25]
	Voltage	Si_3N_4	Cell population	[35]
	Current	Tantalum oxide	DNA/Protein	[36]
	Voltage	Si_3N_4	DNA	[37]

when interacting with biologically sensitive elements and hence do not produce electrical charge. For measuring passive electrical components, different interface circuits are required to convert the changes in biological analytes into measurable voltages or currents. The interface circuits (ie, readout circuits) for these sensors are discussed in the next section.

The resistive-type sensors measure strain-related mechanical properties such as strain, force, acceleration, and pressure-utilizing piezoresistive properties of sensitive film resistors [2,14,38,39]. These sensors are also incorporated as biosensors for detecting biomolecules. The electrode configuration is the same as in electrochemical transducers, but it measures the change of resistance when biomolecules interact with the biologically sensitive elements [2]. The piezoresistive microcantilever sensors are also extensively studied for biosensing. The piezoresistive sensors,

which are covered by a biologically sensitive layer, are bent due to strain induced upon binding of biomolecules with a sensitive layer. The bending of piezoresistive sensors produces a change in resistance [14,38]. Piezoelectric sensors are similar to piezoresistive sensors in which the strain-induced mechanical bending or force produces electrical charge.

The capacitive sensors convert the variations of physical, chemical, and biological quantities into capacitive changes utilizing two electrodes or plates separated by a dielectric medium. For simple capacitors composed of two parallel plates of an area A each, separated by a gap G, and filled with dielectric medium with relative permittivity of ε_r, the capacitance C is expressed as $\varepsilon_0\varepsilon_r A/G$. Here, ε_0 is the permittivity of free space (8.854×10^{-12} F/m). Therefore, a change in the capacitance of the sensing device will occur due to the change of dielectric medium, gap, or area. The capacitive biosensors designed to detect the changes of dielectric medium are very common [40]. The electrodes are configured as parallel plates, coplanar electrodes, and interdigitated electrodes (Fig. 7.4). The parallel-plate configuration requires two metal-printed substrates and the dielectric medium is in between the substrates. The coplanar electrode configuration provides simple fabrication steps compared to the parallel-plate configuration as the electrodes are on the same side of a single substrate. The inter-digitated electrodes configuration is achieved by replicating several coplanar electrode configurations. The capacitive biosensors provide low thermal noise and thermal drift levels, low static power dissipation, and low self-heating [41].

The inductive sensors measure the changes of inductance due to the alteration of magnetic property of the medium. The biomolecules are usually not magnetically sensitive, and therefore, the target molecules are labeled and attached by magnetic particles to have the ability to modify the medium under exposure [42]. Some design examples of these electrical passive transduction techniques are given in Table 7.2.

In addition to sensing techniques, it is also necessary to have a range of selective and sensitive detection of analytes for different applications. The selectivity for specific analytes is one of the most critical requirements for biosensors as it yields reliable

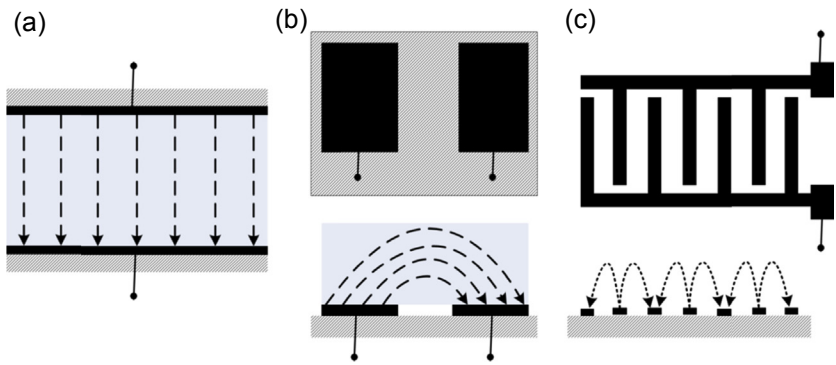

Figure 7.4 The electrode configuration for the capacitive biosensors: (a) parallel plates, (b) coplanar electrodes, (c) interdigitated electrodes.

Table 7.2 The electrical passive transduction techniques

Technique	Sensor output	Circuit output	Configuration	Application	References
Resistive	Resistance	Voltage	Piezoresistive microcantilever	DNA detection	[38]
	Resistance	Frequency	Coplanar electrodes	*E. coli* bacteria	[39]
	Resistance	Voltage	Piezoresistive microcantilever	*Herpes simplex* -1 virus *E. coli* bacteria	[14]
	Resistance	Current	Polymer	Glucose	[43]
Capacitive	Capacitance	Voltage	Interdigitated electrodes	*E. coli* bacteria	[44]
	Capacitance	Digital (8-bit)	Interdigitated electrodes	Dichloro-methane Acetone Methanol Deionized water	[45]
	Capacitance	Voltage	Parallel plates	DNA	[46]
	Capacitance	Frequency	Interdigitated electrodes	pH of gastric acid	[47,48]
Inductive	Inductance	Frequency	Spiral inductor	DNA	[42]

sensing signals in the presence of interfering analytes. The biosensors are developed using biologically sensitive elements such as antibodies and ligands for biological analytes, or metal–organic framework materials for chemical analytes. In addition to the sensing, the sensors are also integrated in systems for immobilizing, analyzing, and identifying chemical and biological analytes.

7.2.2 Readout circuits

Interface circuits for MEMS sensors play an important role for the development of reliable, low-cost, and low-power sensor systems. These signal-conditioning circuits convert the changes of sensor resistance, capacitance, or inductance into equivalent measurable quantities of voltage or current [49,50].

The change in resistance can be measured using a Wheatstone bridge circuit that produces an output voltage proportional to the resistance changes. Another simple way to measure resistance changes as voltage changes is by applying a constant current source through the resistor sensor [14]. The resistance changes of the sensor can also be converted to frequency variations using a voltage-controlled oscillator circuit [51].

There are several readout circuit configurations interfacing with capacitive or inductive sensor systems. The two major circuit configurations are the amplifier-based circuits [49,50,52,53] and modulation-based circuits [15,42,48,51,54–66]. The amplifier-based circuits can be generalized into three categories of alternating current (ac)-bridge [49,53], transimpedance [67], and switched-capacitor (SC) configuration [49,50,52]. In most cases, a single sensing capacitor (C_S) is connected in series with a fixed-reference capacitor (C_R). Capacitor C_R is equal to the rest or initial capacitance of C_S. The C_R and C_S are driven by a differential (180° phase shift) square waves or digital pulses for ac-bridge and switched-capacitor configurations. In transimpedance configurations, an ac-signal (sine wave) is applied. These circuits measure voltage change proportional to the sensor capacitance change ($\Delta C = C_S - C_R$), and the voltage change is amplified using an amplifier circuit. In SC configurations, the amplifier circuit also integrates additional charge from a feedback capacitor at a certain sampling frequency with the sensor capacitance change (ΔC) to minimize the input parasitic capacitance effect. The resolution of SC circuit improves for higher sampling frequencies [49]. The amplified voltage is passed through a low-pass filter to filter out high-frequency components. Various noise sources, such as $1/f$ noise (flicker noise), thermal noise (white noise), substrate–noise coupling (coupled signal from one node to another via the substrate), and parasitic capacitances minimize the sensor readout range and resolution of these circuits [49]. These circuits require lower parasitic capacitance and higher amplitude of input differential signals for the improved range and resolution.

Modulation-based readout circuits have gained popularity for interfacing with capacitive and inductive MEMS sensors to reduce the noise levels of $1/f$ noise and direct current (dc) offset in the circuit. Modulation-based circuits are based on sigma–delta ($\Sigma\Delta$) converter [56,62,65], successive approximation register (SAR) analog-to-digital converter (ADC) [56,66], chopper modulation [54,55,58], pulse-width modulation (PWM) [57,61,63], and frequency modulation (FM) configurations [42,48,51,64,68].

Readout circuits using $\Sigma\Delta$ converters require much faster analog circuits as the sampling rate should much higher than the effective bandwidth, and a digital decimation filter is also needed which adds additional complexity. Moreover, the voltage dependence nonlinearity effect of capacitors results in a lower signal-to-noise ratio (SNR) [60]. Though several nonlinearity compensation techniques have been adopted to adjust the operating point of the CMOS transistors, it is still difficult to maintain the linearity of capacitors with lower supply and bias voltages [60].

An SAR ADC provides a digital output by comparing the analog sensor signal with a sequentially generated analog signal using digital-to-analog (DAC) converter using binary search algorithm [56,66]. This technique consumes lower power and provides high resolution and accuracy.

The chopper modulation approach is an amplitude modulation technique, which uses square wave as a carrier signal. It works by shifting the sensor signals to higher frequencies to suppress the $1/f$ noise. The demodulation of modulated sensor signal is required to recover the original signal [51,58]. Offset and noise compensation should be performed for better performance [51,58].

PWM-based interface circuits exploit semidigital approach in which the capacitance changes are encoded in the time domain and modulated as the period or pulse

width of a digital signal [15,57,61,63]. This technique requires a fast digital counter to convert the time or pulse-width variation into a digital output [59].

The FM configuration that uses oscillator-based reactance sensors detects the frequency shifts introduced by the capacitance or inductance changes of the sensor front-ends [42,48,51,64,68]. These configurations present the advantage of having lower phase and flicker noises at higher frequencies [51,64]. The most common FM circuit for interfacing with capacitive sensors is a relaxation oscillator. A ring oscillator [68,69]-based FM circuit is used in the interface of capacitive sensors, such as a capacitive pressure sensor [68] and a humidity sensor [69]. For the interface of inductive sensors, a Colpitts oscillator topology is adopted to measure nanoscale displacements as a frequency shift in [70]. An integrated complementary cross-coupled oscillator with on-chip LC resonator is investigated in [42,64] for magnetically labeled biosensors and is able to provide highly stable and lower-phase noise output frequency. A low-power FM-demodulation circuit that converts frequency to voltage is also required to measure a voltage quantity. For the implementation of a frequency-to-voltage converter (FVC) block, there are mainly two approaches, including counter-based circuits [68] and integrator-based circuits [71,72]. The counter-based circuits use counters and digital-to-analog converters (DAC) requiring a very high reference-clock frequency compared to the measured signals for high accuracy. The need for a high-frequency clock limits the usage for high-frequency measuring signals [71]. The integrator-based circuits include different approaches such as integrating and holding [72] and switched capacitor [71,72]. Because most of the literature incorporated an FVC block in the design of phase-locked loops (PLLs) or frequency-locked loops (FLLs) as a feedback path for the demodulation of FM signals, it involves higher power requirements. A stand-alone FVC circuit that does not require another oscillator in the feedback loop is also presented to minimize the overall power consumption [73]. The circuit is designed with a negative feedback system, which is based on an integration-based switched-capacitor charge pump circuit. The circuit also provides the control over the sensitivity, dynamic range, and nominal point for the measurement.

7.2.3 Design example of pH sensor and readout circuit

The pH scale measures the acidity or basicity of a substance based on the concentration of hydrogen ions. Due to the pH-dependent nature of several chemical and biological processes, it is frequently necessary to measure the pH for the characteristics of chemical and biological substances. Growing interest in personalized health monitoring has also attracted significant attention to pH measurements in medical science. Local pH measurements in the human body are of significant importance as the changes in pH level in blood, tissues, and other body liquids are an indicator of certain diseases. Therefore, it can provide a timely diagnosis of disease. The pH levels for a healthy tissue lie in the range of 7.2 to 7.6 [74], whereas for the tumor cells, the pH decreases to the acidic side of the neutral level, down to 6.8 [75].

Acidity measurements throughout the digestive system also provide valuable information. The digestive fluid in the stomach, also known as gastric acid, has a usual pH

level of 1 to 2 which is believed to function as a protective mechanism against ingested pathogens [76]. A discrepancy in the pH level of the gastric acid secretion indicates certain disease states [6]. High acidity is generally observed in patients with ulcer, whereas lower level of acid can be an indication of atrophic gastritis and stomach cancer [77]. Conventional methods of measuring the pH of gastric acid are to stimulate gastric secretion by injecting gastric content through a tube placed in the stomach. These methods are time-consuming and uncomfortable [6,78]. Several alternate approaches including endoscopic methods, serum pepsinogens assay, scintigraphic techniques, impedance tomography, alkaline tide, urinary analysis, and breath analysis have been investigated for the measurement of gastric acid [6]. Though these approaches have their own limitations, it is not possible to integrate these approaches with wireless capsules (ie, electronic pills) due to their large-size requirement. Moreover, the wireless capsules can be used as a catheter-free pH detection [79]. They have demonstrated pH measurements with higher sensitivity and resolutions within pH levels of 1.0 to 4.0 [80,81].

Over the years, pH measurement techniques have been evolved from traditional methods, such as pH test strips, potentiometric [31,82–85], and glass electrodes-based [23], to more sophisticated methods including conductometric [86], magnetoelastic [87], optical fiber [88], microcantilever-based systems [89–91], ion-sensitive field-effect transistors (ISFET) [24–27,92,93], and capacitive [47,48]. The glass electrodes-based methods are electrochemical transduction methods that detect pH in a sensing half-cell by measuring the voltage difference between the sensing electrode of the sensing half-cell and a reference electrode having a fixed concentration of HCl or a buffered chloride solution. The voltage difference is generated due to the exchange of sodium ions in the reference half-cell for H^+-ions in the sensing half-cell through a glass membrane [23]. Although the glass electrode method is the standard measuring method for pH due to ideal Nernstian response independent of redox interferences, it shows sluggish response, causes inconsistent results in HF or alkaline solutions, requires conducting sensing materials, and presents unstable responses for miniaturized systems [23]. Potentiometric electrodes can measure the redox reaction potential difference between a reference electrode and pH-sensing metal-oxide electrode, such as PtO_2, IrO_2, TiO_2, SnO_2, Ta_2O_5, RuO_2, RhO_2, and OsO_2 [31,75,82–84]. This method depends on the Nernstian response of redox reactions at solid–liquid interface and can achieve the maximum Nernstian sensitivity of 59.16 mV/pH.

A pH measurement technique based on capacitance changes resulting from permittivity changes as a function of pH is presented in [47,48]. In contrast to the above techniques, this technique can be implemented using interdigitated electrode (IDE)-based sensors, which is suitable to integrate into a miniaturized electronic pill system due to simple structural design and inexpensive fabrication process. The design of IDEs consists of two comb-like electrodes structure on a wafer and the sensing material on top of the electrodes. The amount of H^+-ions, depending on pH values on the sensing materials, change the dielectric permittivity for the fringe electric fields from electrodes. This provides an overall capacitance change for pH change.

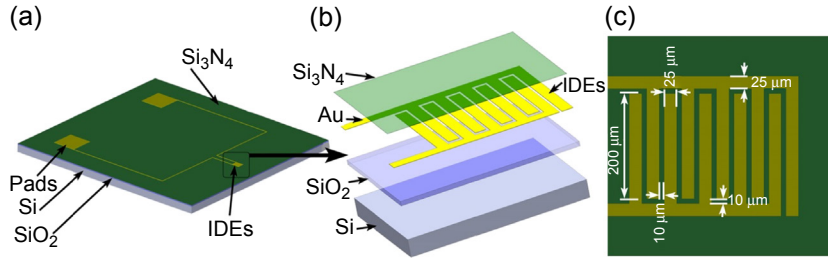

Figure 7.5 (a) Schematic illustration of the microelectromechanical systems (MEMS) fringe-field capacitive pH sensor. (b) Schematic of the multilayered pH sensor fabricated on silicon wafer. (b) Schematic of the IDEs.
M.S. Arefin, M.B. Coskun, T. Alan, J.-M. Redoute, A. Neild, M.R. Yuce, A microfabricated fringing field capacitive pH sensor with an integrated readout circuit, Applied Physics Letters, 104 (2014) 223503.

The MEMS pH sensor detects pH levels by measuring pH-induced permittivity changes in the interdigitated electrodes (IDEs) (Fig. 7.5) [47,48]. In Fig. 7.5(a), the schematic of the sensor is illustrated in three dimensions. The IDEs and pads are fabricated on a silicon (Si) substrate covered with a 500 nm silicon oxide layer. As represented in the exploded view of the sensor in Fig. 7.5(b), the top surfaces of IDEs are passivated by 5 nm thickness of silicon nitride (Si_3N_4) layer to provide a sensing surface for pH buffer solutions as well as to limit Faradaic currents between the electrodes. The IDEs, having each electrode width of 25 µm and length of 200 µm, and interelectrode spacing of 10 µm, are illustrated in Fig. 7.5(c).

In the solution bulk, an electric double-layer capacitance and a diffuse-layer capacitance is formed due to the free H^+-ions in the solution [94,95]. An electric double-layer of H^+-ions forms at the nitride–solution interface that depends on the concentration of H^+-ions of the solutions [94]. The surface charges on the nitride layer act as a source or sink for the H^+-ions in the solutions. In the diffuse layer, the dielectric properties of the solution are modified predominantly by electronic and orientational polarizations under the influence of the high-frequency electric fields. The electronic polarization distorts the electron clouds with the nucleus, whereas the orientational polarization accounts for the reorientation and redistribution of electrical dipoles [95]. Depending on the H^+-ion concentrations, the combined effects of these polarizations alter the relative permittivity (ε_{pH}) of the solutions. The higher concentration of H^+-ions attenuates the external electric fields due to the higher local electric field around the ions and, thus, orients the dipolar water molecules in its vicinity. Hence, lower pH values decrease ε_{pH}. Moreover, the changes in H^+-ions concentrations yield the changes in conductivity (σ_{pH}) of the solution that produce frequency (ω)- dependent complex permittivity $\varepsilon^*_{pH} = \varepsilon_{pH} + j\sigma_{pH}/\omega\varepsilon_0$. Therefore, the change of frequency-dependent dielectric constant for different pH levels is reflected as a change in the capacitance of the sensor.

The capacitance of such a multilayered structure, as shown in Fig. 7.5, having low layer thickness is very difficult to study either by modeling or by finite element method analysis [96]. However, if there is a monotonic increase in permittivity of the layers in the direction of the electrodes' plane to outer medium, the total capacitance of the sensor can be evaluated with the contribution of each layer in series as [96]:

$$C_{\text{sen}} = \frac{N}{2}\left(\frac{C_{\text{ox}}C_{\text{si}}}{C_{\text{ox}}+C_{\text{si}}} + \frac{C_{\text{pH}}C_{\text{n}}}{C_{\text{pH}}+C_{\text{n}}}\right) \tag{7.1}$$

in which C_{sen} is the total sensor capacitance, N is the number of electrodes, and C_{ox}, C_{si}, C_{pH}, and C_{n} are the capacitance contributions from silicon dioxide layer, silicon wafer, pH-buffer solutions, and the silicon nitride layer, respectively. Here, C_{pH} includes the effect of double-layer and diffused-layer capacitance. The sensor under the high-frequency electric fields exhibits an equivalent circuit of the series-connected inductor and sensor capacitance, C_{sen}. The inductance originates from the wired connection of IDEs to pads. At lower frequencies, the capacitance from IDEs is dominant. As the frequency increases, the inductive reactance becomes dominant and cannot provide reactance change for pH change. Therefore, the frequency of operation for the sensor is required to optimize for higher capacitance change.

The capacitive sensor transforms the pH variation to a capacitance change (ΔC). A differential cross-coupled voltage-controlled oscillator (VCO), as shown in Fig. 7.6, is implemented to convert the capacitive variations (ΔC) into frequency variation (ΔF). The differential cross-coupled VCO consists of negative transconductances as well as an inversion-MOS (I-MOS) varactor (C_0) [97] and inductor (L_0) acting as an LC-tank

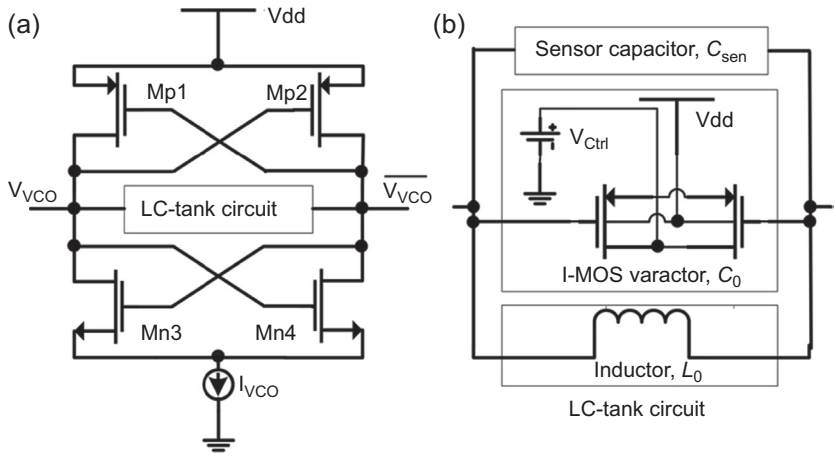

Figure 7.6 (a) Schematic of cross-coupled differential VCO circuit with LC-tank circuit. (b) The LC-tank circuit with the capacitive pH sensor in parallel.
M.S. Arefin, M.B. Coskun, T. Alan, J.-M. Redoute, A. Neild, M.R. Yuce, A microfabricated fringing field capacitive pH sensor with an integrated readout circuit, Applied Physics Letters, 104 (2014) 223503.

of the VCO. A MEMS sensor, C_{sen} is coupled parallel to LC-tank of the VCO to modulate the output frequency. The VCO oscillation frequency can be approximated as $F_{vco} = 1\Big/\left(2\pi\sqrt{L_0\left(C_0 + C_{sen}\right)}\right)$. If the nominal frequency of the oscillator is F_0 for $C_{sen} = 0$ pF, the frequency of the oscillator for the MEMS capacitor, C_{sen} is given by $F_{vco} = F_0\left(1 - C_{sen}/2C_0\right)$ [48,64].

The capacitance of the sensor for the variation of pH obtained from a Vector Network Analyzer (VNA) at 100 MHz is shown in Fig. 7.7. From the figure, the capacitance at pH 1.0 is 7.84 pF that increases by approximately five times and reaches 37.41 pF at pH 5.0. For lower pH, higher concentration of H^+-ions produces lower diffuse-layer capacitance due to higher local electric fields that orient the water molecules in its directions. At very high frequencies, the inductive reactance becomes dominant over the capacitive reactance, hence, the operating frequency of the sensor is kept below 100 MHz.

The sensor is connected to the VCO and the resonant frequency shifts are obtained using a spectrum analyzer. The frequency output of the VCO to corresponding pH values for pH 1.0 to 4.0 is 30.96 MHz that corresponds to a total 31.6% change (Fig. 7.8). Because the molar concentrations of H^+-ions are higher in a strongly acidic region, the sensitivity is very high at low pH levels. The sensitivity for pH 1.0 to 3.0 is 14.335 MHz/pH. The rate of change of resonant frequency decreases for pH 3.0 to 5.0 due to decrease in the molar concentration of H^+-ions. The sensitivity is 1.32 MHz/pH for pH 3.0 to 4.0 and 0.35 MHz/pH for pH 4.0 to 5.0. The magnitudes of the changes for pH 3.0 to 5.0 are still detectable. Similarly, OH^--ion concentrations are higher for a strongly basic region that leads to a larger change as the pH increases, as shown in Fig. 7.8 (inset). Total frequency shift within pH 10 to12 is 4.317 MHz.

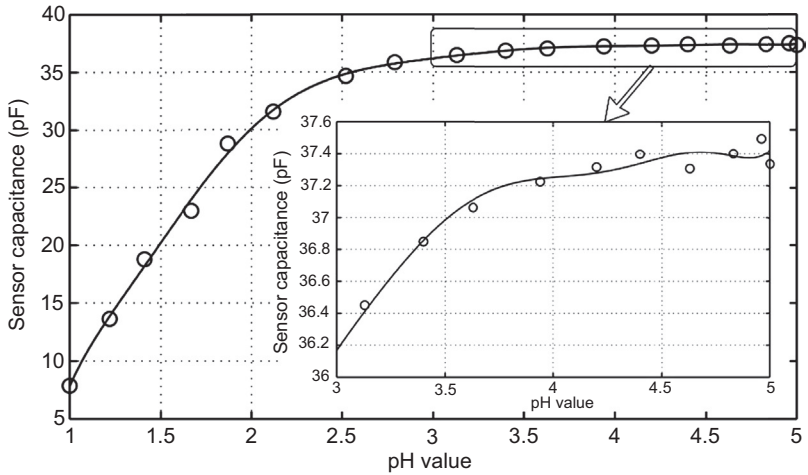

Figure 7.7 The capacitance of the sensor for pH ranging from 1.0 to 5.0 obtained from Vector Network Analyzer (VNA) at 100 MHz. In the inset, the capacitance of the sensor for pH ranges from 3.0 to 5.0.
M.S. Arefin, M.B. Coskun, T. Alan, J.-M. Redoute, A. Neild, M.R. Yuce, A microfabricated fringing field capacitive pH sensor with an integrated readout circuit, Applied Physics Letters, 104 (2014) 223503.

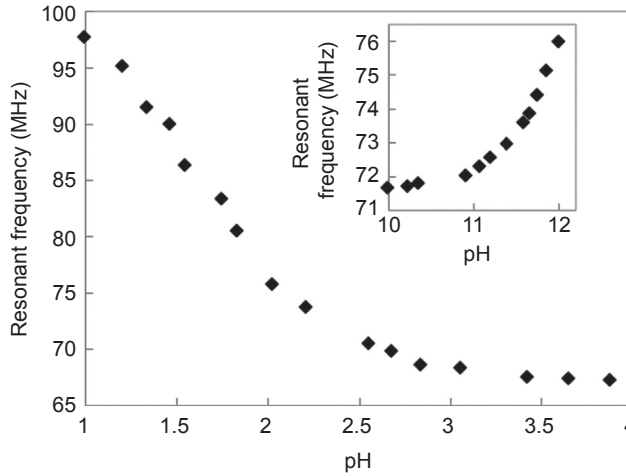

Figure 7.8 The resonance frequency of a voltage-controlled oscillator (VCO) for strong acidic buffer solutions (pH 1–4) and strong basic buffer solutions (pH 10–12) in the inset. M.S. Arefin, M.B. Coskun, T. Alan, A. Neild, J.-M. Redoute, M.R. Yuce, A MEMS capacitive pH sensor for high acidic and basic solutions, in: Proceedings of the IEEE Sensors Conference, 2014, pp. 1792–1794.

In this design example, a capacitive technique has been exploited to measure strong acidic and basic mediums. Such sensors can be integrated within the wireless capsule to measure pH of gastric acid. This technique provides higher sensitivity and low noise readout system while maintaining simple and low-cost fabrication process.

7.3 Wireless telemetry systems

Power consumption is limited in wireless biosensor systems. To prolong the lifetime of biosensors, it is necessary to reduce the power consumption. However, this adds an additional challenge to the digital signal processor (DSP) for supporting radio-frequency (RF) transmissions. Self-powered wireless biosensors are preferred in applications in which sensors are implanted, because, once implemented, it is impractical to access the sensor to recharge the battery. The block diagram of a conventional wireless telemetry system is illustrated in Fig. 7.9. The transmitter circuit is composed of an oscillator, modulator, and a power-amplifier circuit. The modulator processes the measurement data at the operating frequency of the oscillator. The power of the modulated signal is amplified using a power-amplifier (PA) circuit. Finally, the modulated signal is transmitted through antenna via a matching network. The received signal from the antenna and matching network circuit is amplified using a low-noise amplifier (LNA) circuit. The signal is demodulated and filtered to acquire the received data.

For implantable devices, available transmission frequencies compose the medical implant communication services (MICS) band between 402 and 405 MHz, ultrahigh frequency (UHF) 433 MHz or lower-frequency bands including very-high frequency

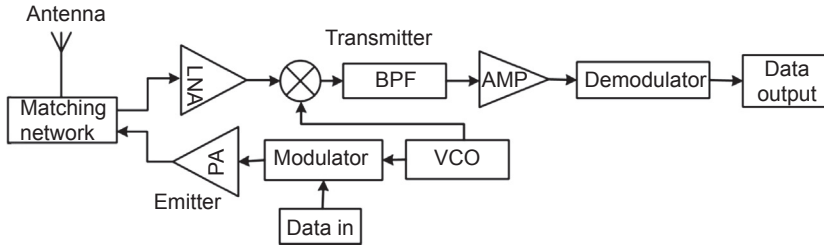

Figure 7.9 Block diagram of a conventional wireless telemetry system.

(VHF) (174–216 MHz) range [40,81,98]. Most of the designs prefer low-frequency transmission due to the inherent high efficiency of transmission through skin layers. As the carrier frequency increases, the attenuation of a wireless signal increases exponentially due to the surrounding tissue [99,100]. This leads to a higher required transmission power. However, lower-frequency transmission requires a larger antenna and occupied space in a wireless capsule. Therefore, there is a trade-off between antenna size and carrier frequency [100].

A simplex telemetry system is employed for the transmission using straightforward modulation schemes such as amplitude modulation, on–off keying, amplitude-shift keying, and phase-shift keying [101–103]. Because the physiological signals vary slowly, such modulation schemes are preferable for miniaturized and low-power wireless biosensors.

For wearable devices, there are several communication technologies to transmit and receive data including MICS, Bluetooth, ultrawide band (UWB), ZigBee, and wireless local area networks (WLAN) [104–111]. Bluetooth operates in the 2.4 GHz ISM bands communicating within seven other devices in a piconet [108]. UWB operates in the 0–960 MHz and 3.1–10 GHz bands [111]. Zigbee operates on a single channel in the 868 MHz, 915 MHz, and 2.4 GHz bands [108]. WLAN follows the Institute of Electrical and Electronics Engineers (IEEE) 802.11 standard describing the physical and Media Access Control (MAC) layer protocol [104,108].

7.4 Applications

Recent progresses in micro- and nanotechnology have led to the design of implantable, swallowable, wearable, or portable wireless biosensors to continuously monitor and detect important physiological parameters. The miniaturization and integration of biosensors, readout circuits, embedded microcontrollers, and wireless transceivers on a single chip have opened the way for new possibilities in medical applications.

7.4.1 Wireless implantable glucose biosensors

Implantable glucose sensors with interface circuits hold a great potential for the continuous measurement and monitoring of blood glucose in patients with diabetes. The sensor can be implanted under the skin [4,33,34,43,112].

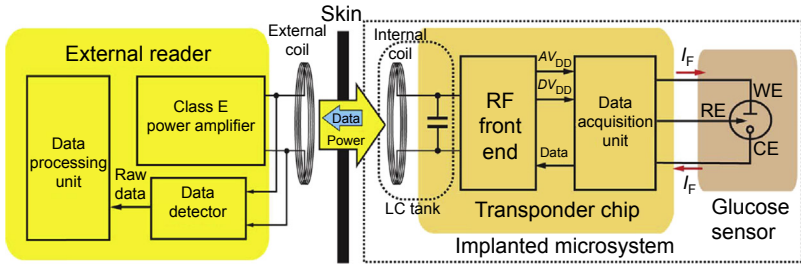

Figure 7.10 Block diagram of the implantable microsystem for continuous glucose monitoring.
M.M. Ahmadi, G.A. Jullien, A wireless-implantable microsystem for continuous blood glucose monitoring, IEEE Transactions on Biomedical Circuits and Systems 3 (2009) 169–180.

The functional block diagram of an implantable microsystem for blood glucose monitoring designed by Ahmadi and Jullien is shown in Fig. 7.10 [34]. The glucose sensor is an amperometric electrochemical biosensor generating a current from the electrochemical reaction between glucose and a glucose oxidase layer on working electrode (WE). The use of iridium-oxide nanoparticles helps for the transfer of the electrons from the glucose oxidase to WE. The reference electrode (RE) eliminates the potential arising from the solution medium. The counter electrode (CE) acts as a reference half-cell to supply the required current for the electrochemical reaction, whereas the WE act as a sensing half-cell to produce the current. The external reader inductively transfers power to the implantable microsystem and receives the transmitted measurement data of blood glucose concentration from the microsystem. The data transmission is performed for every 10 min using a load-shift keying modulation scheme. The interface circuit of the microsystem consists of an RF front-end circuit for receiving RF signals, rectifying, and generating the supply voltage, and a data acquisition circuit for converting the current from glucose sensor to pulse.

The cross-sectional view of the glucose biosensor is illustrated in Fig. 7.11. The titanium–nickel–gold–titanium metallization is essential for the WE, CE, interconnect traces, and bonding pads. The glucose oxidase on gold acts as a biologically sensitive layer. The silver metal layer at RE acts as an Ag/AgCl electrode, which generates current from the solution medium. The integrated interface circuit and the wireless transmitter are bonded on this wafer. The off-chip components and inductive coil for energy transmission are connected on this wafer. The dimension of the microsystem is 8 mm × 4 mm and its thickness is 1 mm.

7.4.2 Wireless capsules

Wireless capsule devices are used in the GI tract to measure physiological parameters. They can monitor motility of the GI tract as a pressure change and transmit the data using low frequencies [40,81]. A summary of previously reported wireless capsules is listed in Table 7.3.

A typical block diagram of wireless capsule system is depicted in Fig. 7.12. The system contains several sensors with analog readout circuits, digital microcontroller

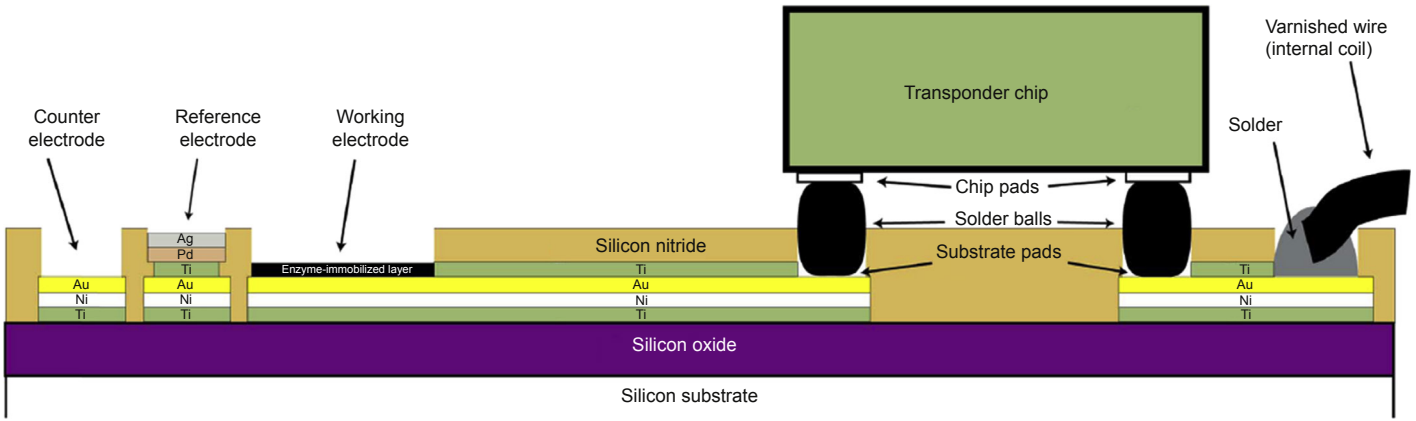

Figure 7.11 Cross-sectional view of the implantable microsystem and glucose sensor for continuous blood glucose monitoring.
M.M. Ahmadi, G.A. Jullien, A wireless-implantable microsystem for continuous blood glucose monitoring, IEEE Transactions on Biomedical Circuits and Systems 3 (2009) 169–180.

Table 7.3 Summary of wireless capsule devices

Capsule name	Capsule dimensions	Sensors	Range	Wireless transmitter	Power source	References
Gutnic	28 mm × 9 mm	pH Pressure Temperature	– – –	–	Gold and Iron electrode battery	[114,115]
Weyrad electronics Ltd.	10 mm × 15 mm	Pressure	0–24.13 kPa	–	Mercury cell battery	[116]
Heidelberg pH capsule	20 mm × 8 mm	pH	1–7	–	Saline activated battery	[117]
Rigel research Ltd.	8.8 mm × 6 mm	Pressure	0–40 kPa	250–570 kHz	Mercury battery	[118]
CorTemp	8.8 mm × 6 mm	Temperature	–	–	Silver oxide battery	[119,120]
Integrated Diagnostics for Environmental and Analytical Systems (IDEAS) (prototype)	55 mm × 16 mm	pH Temperature Conductivity Dissolved oxygen	4–10 0–70°C 0.05–10 mS/cm 0–8.2 mg/L	38.342 MHz (frequency shift keying, FSK)	Silver oxide battery	[101–103]
Bravo pH system	26 mm × 6.3 mm	pH	1.68–7.0	433 MHz	–	[121,122]
Smart pill	22 mm × 9.6 mm	pH Pressure Temperature	– – –	–	Battery	[123]
LIAP	36 mm × 12 mm	pH Temperature	1–10 10–50°C	433.92 MHz (on–off keying, OOK)	Silver oxide battery	[113]

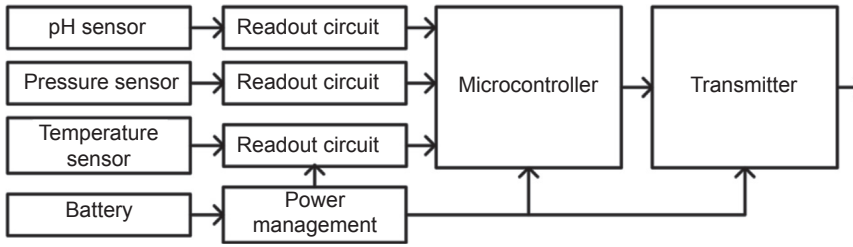

Figure 7.12 The block diagram of a wireless capsule system with biosensors, readout circuits, and transmitter.

circuits, a radio transmitter, and a battery. The sensors convert the physiological parameters to electrical parameters. The controller circuits manage and process all the sensor data. The data from the GI tract is transmitted to an external device for monitoring and recording. The main feature of the system is the integrated multisensor of a pH, pressure, and temperature sensor for real-time signal monitoring of the GI tract abnormalities.

The architecture of a wireless capsule system named the lab-in-a-pill (LIAP) is presented in Fig. 7.13 [113]. It consists of pH and temperature sensors and a custom-made application-specific integrated readout circuit. The pH sensor is a microfabricated ISFET with Ag/AgCl reference electrode. The temperature sensor is an n-channel silicon diode. The system consumes 15.5 mW. The circuit has a power saving feature to operate it for 42 h.

A wireless capsule can provide an invasive method for the diagnosis of the GI tract. The sensor systems for a wireless capsule are composed of mechanical sensors for pressure and position measurement, chemical sensors for pH, conductivity, and dissolved oxygen measurement, and biosensors for bleeding and pathogens detection. In addition to the sensor systems, interface circuits for the sensors also play an important role for the development of low-noise and low-power sensor systems. As a result, wireless capsule requires the development of a reliable, miniaturized, and integrated sensor system with high sensitivity and resolution as well as a low noise, low cost, and a low-power interface circuit system.

7.4.3 Wireless wearable devices

A list of various wireless wearable devices is given in Table 7.4. Different wireless technologies have been used in different wearable devices. A prototype of advanced care and alert portable telemedical monitor (AMON) wrist-worn unit is shown in Fig. 7.14 [8]. The system has two major parts: a wrist-worn unit and a stationary unit at the telemedicine center. The wrist-worn unit measures physiological parameters and transmits through a Global System for Mobile communication (GSM) network to the stationary unit for data collection and processing by trained medical personnel [8]. The stationary unit is composed of a JAVA server platform and a workstation connected to the GSM transceiver.

The functional block diagram of the AMON wrist-worn monitoring unit is shown in Fig. 7.15. The system consists of several sensors, analog readout and

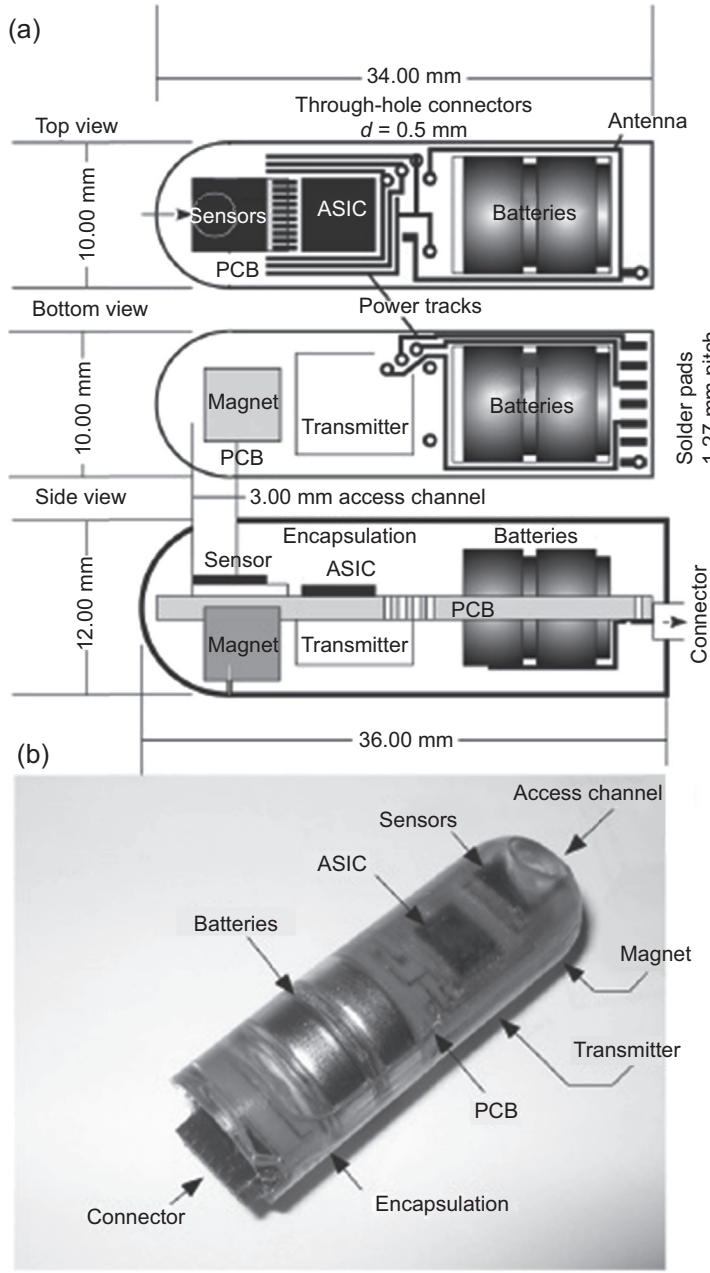

Figure 7.13 The architecture of a wireless capsule containing temperature and pH sensors at the front, followed by application-specific integrated circuit (ASIC) and batteries.
E.A. Johannessen, L. Wang, C. Wyse, D.R. Cumming, J.M. Cooper, Biocompatibility of a lab-on-a-pill sensor in artificial gastrointestinal environments, IEEE Transactions on Biomedical Engineering 53 (2006) 2333–2340.

Table 7.4 List of few wireless wearable devices

Prototype name	Sensors	Wireless Connectivity	Applications	References
AMON	Skin temperature Blood pressure, ECG Blood oxygen Acceleration	GSM	Cardiac/Respiratory patients	[8]
LiveNet	ECG EMG Skin conductance Acceleration	2.4 GHz	Ambulatory health monitoring	[124]
PDA palm-type	ECG PCG Body temperature	Bluetooth	Patient's body condition	[125]
μ-Healthcare system	ECG Blood pressure	IEEE 802.15.4 CDMA	Physiological signal monitoring	[126]
Intrepid	Galvanic skin response Benign positional vertigo Body temperature EMG	Not given	Psychiatric disorder/ anxiety patients	[127]
Not given	ECG Bioimpedance Activity	1 MHz, OOK	Physiological signal monitoring	[9]
Not given	ECG Heart rate Body temperature	Bluetooth	Physiological signal monitoring	[128]

signal conditioning circuits, microcontroller, DSP, communication module, and a display unit. The passive sensors monitor and measure skin temperature, blood pressure, ECG, blood oxygen saturation, and acceleration. The analog readout and signal conditioning circuits are operated for measuring temperature, blood pressure, and ECG. The DSP conditions the ECG and blood pressure signals. The communication module uses a Siemens TC35 Cellular system to connect to the GSM network.

7.5 Conclusion and future trends

This chapter provides an overview of recent developments of implantable and wearable biosensors. Both label-free and label-based biosensors are being studied and developed for detection and measurement of biological parameters. Label-based biosensors

Figure 7.14 A prototype of a wearable medical monitoring device.
U. Anliker, J.A. Ward, P. Lukowicz, G. Troster, F. Dolveck, M. Baer, et al., AMON: a wearable multiparameter medical monitoring and alert system, IEEE Transactions on Information Technology in Biomedicine 8 (2004) 415–427.

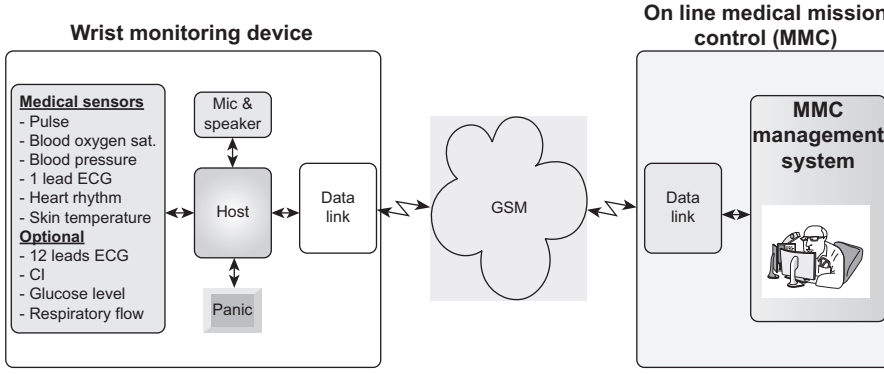

Figure 7.15 System level overview of the wrist-worn medical device with GSM/ Universal Mobile Telecommunication System (UMTS) link.
U. Anliker, J.A. Ward, P. Lukowicz, G. Troster, F. Dolveck, M. Baer, et al., AMON: a wearable multiparameter medical monitoring and alert system, IEEE Transactions on Information Technology in Biomedicine 8 (2004) 415–427.

require fluorescent labels for biomolecules and optical measurement systems, which place some constraints for the use in POC diagnostic devices. Recent POC devices focus on label-free biosensing techniques. The electrochemical and electrical biosensors with interface circuits are very suitable for wireless POC devices. The fundamental elements of these biosensors and the interface or readout circuits are discussed in detail in this chapter. A capacitive pH sensor and interface circuit design to measure gastric acid is presented in detail. Because biosensors are implanted or deployed inside the body, the challenges for smaller size, flexibility, and biocompatibility issues should be addressed. Integrating biosensors and interface circuits with wireless transceivers on semiconductor chips can decrease the size considerably. Because flexible sensors need to be less than 100 μm thick, the challenges to manufacture small and thin biosensors and circuits on chip need to be addressed in the future. Biocompatibility issues are critical for biosensor devices, as the sensitive biomaterial may affect the body adversely as well as degrade over time. Moreover, electrode passivation and interference with other species also limit sensor sensitivity and selectivity. The biocompatible materials for sensors and integrated circuits require expedited advances in the future. It is also crucial to adapt a suitable packaging for the environment into which the biosensors are placed.

Wireless telemetry systems are used to connect biosensor devices to a central node acting as a data acquisition unit. The challenges for such wireless systems are the power radiated through the antenna, the power consumption for data transfer, and the type of network protocol and topology. All the nodes are connected to a central medical database system using the traditional Internet or mobile networks. Three wireless POC systems for implantable and wearable devices are explored to demonstrate the development of wireless integrated sensors functionalized with biologically sensitive elements, integrated interface circuits, and wireless transceiver systems for specific applications. These systems are battery powered, and hence adapting wireless energy harvesting techniques to replace the bulky batteries will lead to new opportunities in the design of biosensors.

The recent developments of the wireless implantable and wearable biosensors for POC applications enable dedicated patient health management. The future trends for POC biosensors outline the need for smaller and flexible integrated systems, new biocompatible materials applicable for different applications, new packaging techniques, energy-efficient wireless systems, improved antenna designs, and efficient wireless power transfer and energy-harvesting techniques.

References

[1] V. Gubala, L.F. Harris, A.J. Ricco, M.X. Tan, D.E. Williams, Point of care diagnostics: status and future, Analytical Chemistry 84 (2011) 487–515.

[2] E. Ghafar-Zadeh, Wireless integrated biosensors for point-of-care diagnostic applications, Sensors 15 (2015) 3236–3261.

[3] Medtronic Inc. Available: http://www.medtronic.com.au/about-medtronic/business-overview/diabetes/index.htm.

[4] N. Sachedina, J. Pickup, Performance assessment of the Medtronic-MiniMed Continuous Glucose Monitoring System and its use for measurement of glycaemic control in Type 1 diabetic subjects, Diabetic Medicine 20 (2003) 1012–1015.
[5] P. Jourand, R. Puers, The BladderPill: an in-body system logging bladder pressure, Sensors and Actuators A: Physical 162 (2010) 160–166.
[6] T. Ghosh, D.I. Lewis, A. Axon, S. Everett, Review article: methods of measuring gastric acid secretion, Alimentary Pharmacology & Therapeutics 33 (2011) 768–781.
[7] M. Chan, D. Estève, J.-Y. Fourniols, C. Escriba, E. Campo, Smart wearable systems: current status and future challenges, Artificial Intelligence in Medicine 56 (2012) 137–156.
[8] U. Anliker, J.A. Ward, P. Lukowicz, G. Troster, F. Dolveck, M. Baer, et al., AMON: a wearable multiparameter medical monitoring and alert system, IEEE Transactions on Information Technology in Biomedicine 8 (2004) 415–427.
[9] T. Vuorela, V.-P. Seppa, J. Vanhala, J. Hyttinen, Design and implementation of a portable long-term physiological signal recorder, IEEE Transactions on Information Technology in Biomedicine 14 (2010) 718–725.
[10] P. Pandian, K. Mohanavelu, K. Safeer, T. Kotresh, D. Shakunthala, P. Gopal, et al., Smart Vest: wearable multi-parameter remote physiological monitoring system, Medical Engineering & Physics 30 (2008) 466–477.
[11] W. Bracke, P. Merken, R. Puers, C. Van Hoof, Ultra-low-power interface chip for autonomous capacitive sensor systems, IEEE Transactions on Circuits and Systems I: Regular Papers 54 (2007) 130–140.
[12] C. Yang, Y. Huang, B.L. Hassler, R.M. Worden, A.J. Mason, Amperometric electrochemical microsystem for a miniaturized protein biosensor array, IEEE Transactions on Biomedical Circuits and Systems 3 (2009) 160–168.
[13] E. Ghafar-Zadeh, M. Sawan, A hybrid microfluidic/CMOS capacitive sensor dedicated to lab-on-chip applications, IEEE Transactions on Biomedical Circuits and Systems 1 (2007) 270–277.
[14] M.S. Arefin, T.L. Porter, An ac electroosmosis device for the detection of bioparticles with piezoresistive microcantilever sensors, Journal of Applied Physics 111 (2012) 054919.
[15] E.Y. Chow, A.L. Chlebowski, P.P. Irazoqui, A miniature-implantable RF-wireless active glaucoma intraocular pressure monitor, IEEE Transactions on Biomedical Circuits and Systems 4 (2010) 340–349.
[16] W.H. Ko, R. Zhang, P. Huang, J. Guo, X. Ye, D.J. Young, et al., Studies of MEMS acoustic sensors as implantable microphones for totally implantable hearing-aid systems, IEEE Transactions on Biomedical Circuits and Systems 3 (2009) 277–285.
[17] V. Espina, E.C. Woodhouse, J. Wulfkuhle, H.D. Asmussen, E.F. Petricoin, L.A. Liotta, Protein microarray detection strategies: focus on direct detection technologies, Journal of Immunological Methods 290 (2004) 121–133.
[18] S. Ray, G. Mehta, S. Srivastava, Label-free detection techniques for protein microarrays: prospects, merits and challenges, Proteomics 10 (2010) 731–748.
[19] P.S. Spuhler, J. Knežević, A. Yalçin, Q. Bao, E. Pringsheim, P. Dröge, et al., Platform for in situ real-time measurement of protein-induced conformational changes of DNA, Proceedings of the National Academy of Sciences 107 (2010) 1397–1401.
[20] K. Ruiz-Mirazo, C. Briones, A. de la Escosura, Prebiotic systems chemistry: new perspectives for the origins of life, Chemical Reviews 114 (2014) 285–366.
[21] H.K. Hunt, A.M. Armani, Label-free biological and chemical sensors, Nanoscale 2 (2010) 1544–1559.

[22] C.T. Lin, P.T.K. Loan, T.Y. Chen, K.K. Liu, C.H. Chen, K.H. Wei, et al., Label-free electrical detection of DNA hybridization on graphene using Hall effect measurements: revisiting the sensing mechanism, Advanced Functional Materials 23 (2013) 2301–2307.
[23] M. Yuqing, C. Jianrong, F. Keming, New technology for the detection of pH, Journal of Biochemical and Biophysical Methods 63 (2005) 1–9.
[24] P. Bergveld, Thirty years of ISFETOLOGY: what happened in the past 30 years and what may happen in the next 30 years, Sensors and Actuators B: Chemical 88 (2003) 1–20.
[25] Y.-H. Chang, Y.-S. Lu, Y.-L. Hong, S. Gwo, J.A. Yeh, Highly sensitive pH sensing using an indium nitride ion-sensitive field-effect transistor, IEEE Sensors Journal 11 (2011) 1157–1161.
[26] J.-C. Chou, S.-I. Liu, S.-H. Chen, Sensing characteristics of ruthenium films fabricated by radio frequency sputtering, Japanese Journal of Applied Physics 44 (2005) 1403.
[27] J. Go, P.R. Nair, B. Reddy Jr., B. Dorvel, R. Bashir, M.A. Alam, Coupled heterogeneous nanowire–nanoplate planar transistor sensors for giant (>10 V/pH) Nernst response, ACS Nano 6 (2012) 5972–5979.
[28] M. Schienle, C. Paulus, A. Frey, F. Hofmann, B. Holzapfl, P. Schindler-Bauer, et al., A fully electronic DNA sensor with 128 positions and in-pixel A/D conversion, IEEE Journal of Solid-State Circuits 39 (2004) 2438–2445.
[29] P.M. Levine, P. Gong, R. Levicky, K.L. Shepard, Real-time, multiplexed electrochemical DNA detection using an active complementary metal-oxide-semiconductor biosensor array with integrated sensor electronics, Biosensors and Bioelectronics 24 (2009) 1995–2001.
[30] T. Yamazaki, T. Ikeda, Y. Kano, H. Takao, M. Ishida, K. Sawada, Design and fabrication of complementary metal–oxide–semiconductor sensor chip for electrochemical measurement, Japanese Journal of Applied Physics 49 (2010) 04DL11.
[31] E. Prats-Alfonso, L. Abad, N. Casan-Pastor, J. Gonzalo-Ruiz, E. Baldrich, Iridium oxide pH sensor for biomedical applications. Case urea–urease in real urine samples, Biosensors and Bioelectronics 39 (2013) 163–169.
[32] L. Li, X. Liu, W.A. Qureshi, A.J. Mason, CMOS amperometric instrumentation and packaging for biosensor array applications, IEEE Transactions on Biomedical Circuits and Systems 5 (2011) 439–448.
[33] L. Meng, Y. Xia, W. Liu, L. Zhang, P. Zou, Y. Zhang, Hydrogen microexplosion synthesis of platinum nanoparticles/nitrogen doped graphene nanoscrolls as new amperometric glucose biosensor, Electrochimica Acta 152 (2015) 330–337.
[34] M.M. Ahmadi, G.A. Jullien, A wireless-implantable microsystem for continuous blood glucose monitoring, IEEE Transactions on Biomedical Circuits and Systems 3 (2009) 169–180.
[35] S. Purushothaman, C. Toumazou, C.-P. Ou, Protons and single nucleotide polymorphism detection: a simple use for the Ion Sensitive Field Effect Transistor, Sensors and Actuators B: Chemical 114 (2006) 964–968.
[36] J.K. Shin, D.S. Kim, H.J. Park, G. Lim, Detection of DNA and protein molecules using an FET-type biosensor with gold as a gate metal, Electroanalysis 16 (2004) 1912–1918.
[37] L. Bandiera, G. Cellere, S. Cagnin, A. De Toni, E. Zanoni, G. Lanfranchi, et al., A fully electronic sensor for the measurement of cDNA hybridization kinetics, Biosensors and Bioelectronics 22 (2007) 2108–2114.
[38] R.L. Gunter, R. Zhine, W.G. Delinger, K. Manygoats, A. Kooser, T.L. Porter, Investigation of DNA sensing using piezoresistive microcantilever probes, IEEE Sensors Journal 4 (2004) 430–433.

[39] L. Yao, P. Lamarche, N. Tawil, R. Khan, A.M. Aliakbar, M.H. Hassan, et al., CMOS conductometric system for growth monitoring and sensing of bacteria, IEEE Transactions on Biomedical Circuits and Systems 5 (2011) 223–230.
[40] K. Arshak, E. Jafer, G. Lyons, D. Morris, O. Korostynska, A review of low-power wireless sensor microsystems for biomedical capsule diagnosis, Microelectronics International 21 (2004) 8–19.
[41] V. Ferrari, M. Prudenziati, 8-Printed thick-film capacitive sensors, in: M. Prudenziati, J. Hormadaly (Eds.), Printed Films, Woodhead Publishing, 2012, pp. 193–220.
[42] H. Wang, Y. Chen, A. Hassibi, A. Scherer, A. Hajimiri, A frequency-shift CMOS magnetic biosensor array with single-bead sensitivity and no external magnet, in: Solid-State Circuits Conference-Digest of Technical Papers, 2009. ISSCC 2009. IEEE International, 2009, pp. 438–439.
[43] E.S. Forzani, H. Zhang, L.A. Nagahara, I. Amlani, R. Tsui, N. Tao, A conducting polymer nanojunction sensor for glucose detection, Nano Letters 4 (2004) 1785–1788.
[44] E. Ghafar-Zadeh, M. Sawan, V.P. Chodavarapu, T. Hosseini-Nia, Bacteria growth monitoring through a differential CMOS capacitive sensor, IEEE Transactions on Biomedical Circuits and Systems 4 (2010) 232–238.
[45] E. Ghafar-Zadeh, M. Sawan, Charge-based capacitive sensor array for CMOS-based laboratory-on-chip applications, IEEE Sensors Journal 8 (2008) 325–332.
[46] J. Musayev, Y. Adlguzel, H. Kulah, S. Eminoglu, T. Akln, Label-free DNA detection using a charge sensitive CMOS microarray sensor chip, IEEE Sensors Journal 14 (2014) 1608–1616.
[47] M.S. Arefin, M.B. Coskun, T. Alan, A. Neild, J.-M. Redoute, M.R. Yuce, A MEMS capacitive pH sensor for high acidic and basic solutions, in: Proceedings of the IEEE Sensors Conference, 2014, pp. 1792–1794.
[48] M.S. Arefin, M.B. Coskun, T. Alan, J.-M. Redoute, A. Neild, M.R. Yuce, A microfabricated fringing field capacitive pH sensor with an integrated readout circuit, Applied Physics Letters 104 (2014) 223503.
[49] N. Yazdi, H. Kulah, K. Najafi, Precision readout circuits for capacitive microaccelerometers, in: Proceedings of the IEEE Sensors Conference, 2004, pp. 28–31.
[50] N. Yazdi, A. Mason, K. Najafi, K.D. Wise, A generic interface chip for capacitive sensors in low-power multi-parameter microsystems, Sensors and Actuators A: Physical 84 (2000) 351–361.
[51] A. Mohammadi, M.R. Yuce, S.R. Moheimani, Frequency modulation technique for MEMS resistive sensing, IEEE Sensors Journal 12 (2012) 2690–2698.
[52] H. Kulah, J. Chae, N. Yazdi, K. Najafi, A multi-step electromechanical/spl Sigma//spl Delta/converter for micro-g capacitive accelerometers, in: Solid-State Circuits Conference, 2003. Digest of Technical Papers. ISSCC. 2003 IEEE International, 2003, pp. 202–488.
[53] J. Wu, G.K. Fedder, L.R. Carley, A low-noise low-offset capacitive sensing amplifier for a 50-μg/√Hz monolithic CMOS MEMS accelerometer, IEEE Journal of Solid-State Circuits 39 (2004) 722–730.
[54] P.K. Chan, J. Cui, Design of chopper-stabilized amplifiers with reduced offset for sensor applications, IEEE Sensors Journal 8 (2008) 1968–1980.
[55] M. Dei, P. Bruschi, M. Piotto, Design of CMOS chopper amplifiers for thermal sensor interfacing, in: Ph. D. Research in Microelectronics and Electronics, 2008. PRIME 2008, 2008, pp. 205–208.
[56] H. Ha, D. Sylvester, D. Blaauw, J.-Y. Sim, 12.6 A 160nW 63.9 fJ/conversion-step capacitance-to-digital converter for ultra-low-power wireless sensor nodes, in: Solid-State Circuits Conference Digest of Technical Papers (ISSCC), 2014 IEEE International, 2014, pp. 220–221.

[57] J.-L. Lu, M. Inerowicz, S. Joo, J.-K. Kwon, B. Jung, A low-power, wide-dynamic-range semi-digital universal sensor readout circuit using pulsewidth modulation, IEEE Sensors Journal 11 (2011) 1134–1144.
[58] J. Nebhen, S. Meillère, M. Masmoudi, J. Seguin, H. Barthelemy, K. Aguir, Low noise micro-power chopper amplifier for MEMS gas sensor, in: Mixed Design of Integrated Circuits and Systems (MIXDES), 2011 Proceedings of the 18th International Conference, 2011, pp. 348–351.
[59] H. Omran, M. Arsalan, K.N. Salama, A 7.9 pJ/Step Energy-Efficient Multi-Slope 13-bit Capacitance-to-Digital Converter, 2014.
[60] J. Sauerbrey, T. Tille, D. Schmitt-Landsiedel, R. Thewes, A 0.7-V MOSFET-only switched-opamp ΣΔ modulator in standard digital CMOS technology, IEEE Journal of Solid-State Circuits 37 (2002) 1662–1669.
[61] M.-L. Sheu, W.-H. Hsu, L.-J. Tsao, A capacitance-ratio-modulated current front-end circuit with pulsewidth modulation output for a capacitive sensor interface, IEEE Transactions on Instrumentation and Measurement 61 (2012) 447–455.
[62] D.-Y. Shin, H. Lee, S. Kim, A delta–sigma interface circuit for capacitive sensors with an automatically calibrated zero point, IEEE Transactions on Circuits and Systems II: Express Briefs 58 (2011) 90–94.
[63] Z. Tan, S.H. Shalmany, G.C. Meijer, M.A. Pertijs, An energy-efficient 15-bit capacitive-sensor interface based on period modulation, IEEE Journal of Solid-State Circuits 47 (2012) 1703–1711.
[64] H. Wang, C.-C. Weng, A. Hajimiri, Phase noise and fundamental sensitivity of oscillator-based reactance sensors, IEEE Transactions on Microwave Theory and Techniques 61 (2013) 2215–2229.
[65] S. Xia, K. Makinwa, S. Nihtianov, A capacitance-to-digital converter for displacement sensing with 17b resolution and 20 µs conversion time, in: Solid-State Circuits Conference Digest of Technical Papers (ISSCC), 2012 IEEE International, 2012, pp. 198–200.
[66] M. Yip, A.P. Chandrakasan, A resolution-reconfigurable 5-to-10-bit 0.4-to-1 V power scalable SAR ADC for sensor applications, IEEE Journal of Solid-State Circuits 48 (2013) 1453–1464.
[67] J.A. Geen, S.J. Sherman, J.F. Chang, S.R. Lewis, Single-chip surface micromachined integrated gyroscope with 50/h Allan deviation, IEEE Journal of Solid-State Circuits 37 (2002) 1860–1866.
[68] E.D. Kyriakis-Bitzaros, N.A. Stathopoulos, S. Pavlos, D. Goustouridis, S. Chatzandroulis, A reconfigurable multichannel capacitive sensor array interface, IEEE Transactions on Instrumentation and Measurement 60 (2011) 3214–3221.
[69] F. Deng, Y. He, C. Zhang, W. Feng, A CMOS humidity sensor for passive RFID sensing applications, Sensors 14 (2014) 8728–8739.
[70] M.B. Coskun, K. Thotahewa, Y.-S. Ying, M. Yuce, A. Neild, T. Alan, Nanoscale displacement sensing using microfabricated variable-inductance planar coils, Applied Physics Letters 103 (2013) 143501.
[71] H.T. Bui, Y. Savaria, Design of a high-speed differential frequency-to-voltage converter and its application in a 5-GHz frequency-locked loop, IEEE Transactions on Circuits and Systems I: Regular Papers 55 (2008) 766–774.
[72] A. Djemouai, M.A. Sawan, M. Slamani, New frequency-locked loop based on CMOS frequency-to-voltage converter: design and implementation, IEEE Transactions on Circuits and Systems II: Analog and Digital Signal Processing 48 (2001) 441–449.
[73] M.S. Arefin, J.M. Redoute, M.R. Yuce, A MEMS interface IC with low-power and wide-range frequency-to-voltage converter for biomedical applications, IEEE Transactions on Biomedical Circuits and Systems 10(2), (2016) 455–466.

[74] J. Griffiths, Are cancer cells acidic? British Journal of Cancer 64 (1991) 425.
[75] X. Zhang, Y. Lin, R.J. Gillies, Tumor pH and its measurement, Journal of Nuclear Medicine 51 (2010) 1167–1170.
[76] T.C. Martinsen, K. Bergh, H.L. Waldum, Gastric juice: a barrier against infectious diseases, Basic & Clinical Pharmacology & Toxicology 96 (2005) 94–102.
[77] S. Kwiecien, S. Konturek, Gastric analysis with fractional test meals (ethanol, caffeine, and peptone meal), augmented histamine or pentagastrin tests, and gastric pH recording, Journal of Physiology and Pharmacology 54 (2003) 69–82.
[78] H.O. Hart, P. Madsen, The effect of tetragastrin on gastric acid secretion. Reproducibility and comparison with the pentagastrin test and the augmented histamine test, Scandinavian Journal of Gastroenterology 7 (1972) 171.
[79] R. Banerjee, D.N. Reddy, Bravo capsule pH monitoring, The American Journal of Gastroenterology 101 (2006) 906.
[80] E. Gill, A. Arshak, K. Arshak, O. Korostynska, Novel conducting polymer composite pH sensors for medical applications, in: 14th Nordic-Baltic Conference on Biomedical Engineering and Medical Physics, 2008, pp. 225–228.
[81] M.R. Yuce, T. Dissanayake, H.C. Keong, Wireless telemetry for electronic pill technology, in: IEEE Sensors 2009, 2009, pp. 1433–1438.
[82] S. Bhadra, C. Dynowski, W. Blunt, M. McDonald, D.J. Thomson, M. Freund, et al., Wireless passive sensor for pH monitoring inside a small bioreactor, in: Instrumentation and Measurement Technology Conference (I2MTC), 2013 IEEE International, 2013, pp. 276–279.
[83] W.-D. Huang, H. Cao, S. Deb, M. Chiao, J.-C. Chiao, A flexible pH sensor based on the iridium oxide sensing film, Sensors and Actuators A: Physical 169 (2011) 1–11.
[84] Y.-H. Liao, J.-C. Chou, Preparation and characteristics of ruthenium dioxide for pH array sensors with real-time measurement system, Sensors and Actuators B: Chemical 128 (2008) 603–612.
[85] R. Zhao, M. Xu, J. Wang, G. Chen, A pH sensor based on the TiO_2 nanotube array modified Ti electrode, Electrochimica Acta 55 (2010) 5647–5651.
[86] W.-S. Han, M.-Y. Park, D.-H. Cho, T.-K. Hong, D.-H. Lee, J.-M. Park, et al., The behavior of a poly (aniline) solid contact pH selective electrode based on *N, N, N', N'*-tetrabenzylethanediamine ionophore, Analytical Sciences 17 (2001) 727–732.
[87] C. Ruan, K. Zeng, C.A. Grimes, A mass-sensitive pH sensor based on a stimuli-responsive polymer, Analytica Chimica Acta 497 (2003) 123–131.
[88] C. Hazneci, K. Ertekin, B. Yenigul, E. Cetinkaya, Optical pH sensor based on spectral response of newly synthesized Schiff bases, Dyes and Pigments 62 (2004) 35–41.
[89] R. Bashir, J. Hilt, O. Elibol, A. Gupta, N. Peppas, Micromechanical cantilever as an ultrasensitive pH microsensor, Applied Physics Letters 81 (2002) 3091–3093.
[90] A. Boisen, S. Dohn, S.S. Keller, S. Schmid, M. Tenje, Cantilever-like micromechanical sensors, Reports on Progress in Physics 74 (2011) 036101.
[91] S.-J. Kim, T. Ono, M. Esashi, Capacitive resonant mass sensor with frequency demodulation detection based on resonant circuit, Applied Physics Letters 88 (2006) 053116.
[92] P.K. Ang, W. Chen, A.T.S. Wee, K.P. Loh, Solution-gated epitaxial graphene as pH sensor, Journal of the American Chemical Society 130 (2008) 14392–14393.
[93] M. Yuqing, G. Jianguo, C. Jianrong, Ion sensitive field effect transducer-based biosensors, Biotechnology Advances 21 (2003) 527–534.
[94] R. Kötz, M. Carlen, Principles and applications of electrochemical capacitors, Electrochimica Acta 45 (2000) 2483–2498.
[95] V.S. Bagotsky, Fundamentals of Electrochemistry, vol. 44, John Wiley & Sons, 2005.

[96] R. Igreja, C. Dias, Extension to the analytical model of the interdigital electrodes capacitance for a multi-layered structure, Sensors and Actuators A: Physical 172 (2011) 392–399.
[97] P. Andreani, S. Mattisson, On the use of MOS varactors in RF VCOs, IEEE Journal of Solid-State Circuits 35 (2000) 905–910.
[98] A. Arshak, K. Arshak, D. Waldron, D. Morris, O. Korostynska, E. Jafer, et al., Review of the potential of a wireless MEMS and TFT microsystems for the measurement of pressure in the GI tract, Medical Engineering & Physics 27 (2005) 347–356.
[99] M.R. Yuce, G. Alici, T.D. Than, Wireless endoscopy, Wiley Encyclopedia of Electrical and Electronics Engineering (December 2014) 1–25.
[100] M.R. Yuce, T. Dissanayake, Easy-to-swallow antenna and propagation, IEEE Microwave Magazine 14 (2013) 74.
[101] E.A. Johannessen, T.-B. Tang, L. Wang, L. Cui, M. Ahmadian, N. Aydin, et al., An ingestible electronic pill for real time analytical measurements of the gastrointestinal tract, in: Proceedings of MTAS 2002 Symposium, 2002, pp. 181–183.
[102] T.B. Tang, E.A. Johannessen, L. Wang, A. Astaras, M. Ahmadian, L. Cui, et al., IDEAS: a miniature lab-in-a-pill multisensor microsystem, in: IEEE NORCHIP Conference, 2002.
[103] T.B. Tang, E.A. Johannessen, L. Wang, A. Astaras, M. Ahmadian, A.F. Murray, et al., Toward a miniature wireless integrated multisensor microsystem for industrial and biomedical applications, IEEE Sensors Journal 2 (2002) 628–635.
[104] P. Madoglio, A. Ravi, H. Xu, K. Chandrashekar, M. Verhelst, S. Pellerano, et al., A 20dBm 2.4 GHz digital outphasing transmitter for WLAN application in 32 nm CMOS, in: Solid-State Circuits Conference Digest of Technical Papers (ISSCC), 2012 IEEE International, 2012, pp. 168–170.
[105] A. Mathew, N. Chandrababu, K. Elleithy, S. Rizvi, IEEE 802.11 & bluetooth interference: simulation and coexistence, in: Communication Networks and Services Research Conference, 2009. CNSR'09. Seventh Annual, 2009, pp. 217–223.
[106] FCC Rules and Regulations, MICS Band Plan, 2003.
[107] V. Shirvante, F. Todeschini, X. Cheng, Y.-K. Yoon, Compact spiral antennas for MICS band wireless endoscope toward pediatric applications, in: Antennas and Propagation Society International Symposium (APSURSI), 2010 IEEE, 2010, pp. 1–4.
[108] P.J. Soh, G. Vandenbosch, M. Mercuri, D.M.-P. Schreurs, Wearable wireless health monitoring: current developments, challenges, and future trends, IEEE Microwave Magazine 16 (2015) 55–70.
[109] M.R. Yuce, S.W. Ng, N.L. Myo, J.Y. Khan, W. Liu, Wireless body sensor network using medical implant band, Journal of Medical Systems 31 (2007) 467–474.
[110] M.R. Yuce, Implementation of wireless body area networks for healthcare systems, Sensors and Actuators A: Physical 162 (2010) 116–129.
[111] M.R. Yuce, H.C. Keong, M.S. Chae, Wideband communication for implantable and wearable systems, IEEE Transactions on Microwave Theory and Techniques 57 (2009) 2597–2604.
[112] B. Yu, N. Long, Y. Moussy, F. Moussy, A long-term flexible minimally-invasive implantable glucose biosensor based on an epoxy-enhanced polyurethane membrane, Biosensors and Bioelectronics 21 (2006) 2275–2282.
[113] E.A. Johannessen, L. Wang, C. Wyse, D.R. Cumming, J.M. Cooper, Biocompatibility of a lab-on-a-pill sensor in artificial gastrointestinal environments, IEEE Transactions on Biomedical Engineering 53 (2006) 2333–2340.
[114] R.S. Mackay, B. Jacobson, Endoradiosonde, 1957.
[115] V.K. Zworykin, A radio pill, Nature 179 (June 1957) 1239–1240.

[116] E.G. Osborne, M.H. Pressly, Endoradiosondes, Weyrad Electronics Ltd., Great Britain, 1973, p. 5.
[117] S. Barrie, Heidelberg pH capsule gastric analysis, in: J.E. Pizzorno, M.T. Murray (Eds.), A Textbook of Natural Medicine, JBC Publications, Seattle, WA, 1992.
[118] S. Kumar, The effect of sustained spinal load on intra-abdominal pressure and EMG characteristics of trunk muscles, Ergonomics 40 (1997) 1312–1334.
[119] P.N. Cutchis, A.F. Hogrefe, J.C. Lesho, The ingestible thermal monitoring system, Johns Hopkins APL Technical Digest 9 (1988) 16–21.
[120] T. Togawa, T. Tamura, P.A. Oberg, Biomedical Transducers and Instruments, CRC Press, 1997.
[121] J.E. Pandolfino, J.E. Richter, T. Ours, J.M. Guardino, J. Chapman, P.J. Kahrilas, Ambulatory esophageal pH monitoring using a wireless system, The American Journal of Gastroenterology 98 (2003) 740–749.
[122] C. Ruan, K.G. Ong, C. Mungle, M. Paulose, N.J. Nickl, C.A. Grimes, A wireless pH sensor based on the use of salt-independent micro-scale polymer spheres, Sensors and Actuators B: Chemical 96 (2003) 61–69.
[123] S.D. Inc., Datasheet, (2004).
[124] M. Sung, C. Marci, A. Pentland, Wearable feedback systems for rehabilitation, Journal of Neuroengineering and Rehabilitation 2 (2005) 1–12.
[125] J.-R.C. Chien, C.-C. Tai, A new wireless-type physiological signal measuring system using a PDA and the bluetooth technology, Biomedical Engineering: Applications, Basis and Communications 17 (2005) 229–235.
[126] W.-Y. Chung, S.-C. Lee, S.-H. Toh, WSN based mobile u-healthcare system with ECG, blood pressure measurement function, in: Engineering in Medicine and Biology Society, 2008. EMBS 2008. 30th Annual International Conference of the IEEE, 2008, pp. 1533–1536.
[127] G. Riva, A. Gorini, A. Gaggioli, The intrepid project-biosensor-enhanced virtual therapy for the treatment of generalized anxiety disorders, Studies in Health Technology and Informatics 142 (2009) 155.
[128] J.-S. Lin, S.-Y. Huang, K.-W. Pan, S.-H. Liu, A physiological signal monitoring system based on an SoC platform and wireless network technologies in homecare technology, Journal of Medical and Biological Engineering 29 (2009) 47–51.